To cope with drought: two forage grass species – Festuca arundinacea and F. glaucescens can activate similar survival strategies although they differ with molecular response

Katarzyna Lechowicz
Institute of Plant Genetics, Polish Academy of Sciences
Izabela Pawlowicz (ipaw@igr.poznan.pl)
Polska Akademia Nauk Instytut Oceanologii https://orcid.org/0000-0002-0790-6599
Dawid Perlikowski
Institute of Plant Genetics, Polish Academy of Sciences
Magdalena Arasimowicz-Jelonek
Uniwersytet im Adama Mickiewicza w Poznaniu Wydzial Anglistyki
Joanna Majka
Institute of Plant Genetics, Polish Academy of Sciences
Adam Augustyniak
Institute of Plant Genetics, Polish Academy of Sciences
Arkadiusz Kosmala
Institute of Botany Chinese Academy of Sciences

Research article

Keywords: Antioxidant enzymes, Drought strategies, Festuca arundinacea, F. glaucescens, ROS, Photosynthesis

Posted Date: December 5th, 2019

DOI: https://doi.org/10.21203/rs.2.18305/v1

Abstract

Background: Photosynthesis is among the primary processes affected by drought and its disturbances result with the reduction of growth, reactive oxygen species (ROS) overproduction, and alterations in antioxidant system activity. Our study was performed on two closely related forage grasses: Festuca arundinacea and F. glaucescens. Two genotypes within each species significantly differing with the potential of drought resistance: high drought resistant (HDR) and low drought resistant (LDR), were used. The research involved: (i) the analysis of gene expression at transcript and protein levels for the selected enzymes of Calvin cycle (fructose-1,6-bisphosphate aldolase (pFBA), phosphoglycerate kinase (PGK) and glyceraldehyde-3-phosphate dehydrogenase (GAPDH)) and (ii) the activity of pFBA, as a protein marker of the Calvin cycle, (iii) the analysis of gene expression at protein level for the selected antioxidant enzymes (glutathione reductase (GR), glutathione peroxidase (GPX), L-ascorbate peroxidase (APX), catalase (CAT), and superoxide dismutase (SOD)), (iv) the measurements of physiological parameters describing a plant's physiological status under control, drought and re-watering conditions (relative water content (RWC), electrolyte leakage (EL), lipid peroxidation, chlorophyll fluorescence, gas exchange, and ROS level).

Results: Our analysis clearly showed that physiological reactions to water deficit were similar in both HDR and both LDR genotypes of Festuca arundinacea and F. glaucescens but the species revealed significant differences in the potential to tolerate tissue dehydration, what was correlated with distinct expression of the Calvin cycle enzymes under drought stress.

Conclusions: The maintenance of stable efficiency of dark phase of photosynthesis seems to be crucial for drought tolerance and recovery in F. glaucescnes, whereas acquisition of drought tolerance in F. arundinacea and F. glaucescens does not involve marked changes at the protein level in the enzymatic antioxidant system.

Background

A lack of water is one of the main environmental factors that affects plant growth and development, and significantly reduces the yield of many crop species with economic importance. Considering rapid climate changes with global warming being the most noticeable, we can expect that periods of drought will occur more often than previously, even in temperate regions (1). Thus, the recognition of cellular mechanisms conferring plant drought resistance seems to be crucial.

Grasslands cover around 70% of the world's agricultural area and are mainly used for fodder purposes (2). Forage grasses belonging to *Lolium* and *Festuca* genera are one of the most important in the temperate regions. Our previous studies revealed that *Festuca* species could be successfully used as models to precisely dissect mechanisms of resistance to a wide range of abiotic stresses in a group of forage grasses (e.g. 3, 4, 5, 6, 7, 8, 9).

Allohexaploid *Festuca arundinacea* Schreb. (2n = 6x = 42) and tetraploid *F. arundinacea* var. *glaucescens* Boiss. (hereafter recognized as *F. glaucescens*) (2n = 4x = 28) are closely related cool-season forage grasses (10) with a relatively high potential to withstand periods of water shortage. In *F. arundinacea*, drought resistance is mostly manifested by a drought avoidance strategy which relies on the development of deep root system, leaf rolling and a rapid stomatal closure (5, 11). However, our earlier experiments revealed that *F. arundinacea* could also develop a drought tolerance strategy mainly associated with the adjustment of leaf metabolism to water deficit in plant tissues (5, 6). On the other hand, *F. glaucescens* was described earlier as a species characterized mainly by a metabolism slowdown and a reduction of growth associated with a quiescence under drought conditions, followed by a further recovery after stress cessation, which enables it to survive and to resume the growth following irrigation (12, 13). The knowledge about molecular basis of drought resistance is strongly limited in this species.

Photosynthesis is among the primary processes to be affected by drought. Its efficiency can be restricted by both stomatal and non-stomatal mechanisms. Stomata closing declines CO_2 availability, whereas among the non-stomatal mechanism, a reduction of Calvin cycle efficiency was indicated to be crucial (8, 14, 15, 16).

Drought, especially the initial phase of stress duration, can also result in the oxidative stress manifested by the reactive oxygen species (ROS) overproduction (17, 18), with hydrogen peroxide (H_2O_2), hydroxyl radical (OH) and superoxide anions ($O_2^{\bullet-}$) being the most severe (19). Although these molecules serve as signals in the numerous processes associated with plant growth and development, ROS are also recognized as key players in stress signaling (20, 21). However, a stress-induced overproduction of ROS can lead to the damage of photosynthetic apparatus and the disturbance of different metabolic pathways (21, 22, 23, 24). Furthermore, the enhanced production of ROS during drought supports lipid peroxidation, and finally contributes to the damage of cellular membranes (25). The ROS-scavenging enzymatic system was proved to be one of the most crucial components of drought resistance in many plant species (26, 27). Moreover, the enzymes contribute to the maintenance of cellular redox balance, particularly during stress response (28, 29, 30). The systems includes glutathione reductase (GR), glutathione peroxidase (GPX), L-ascorbate peroxidase (APX), catalase (CAT), and superoxide dismutase (SOD). Superoxide dismutases are classified according to their metal cofactor, and among them, Fe-dependent superoxide dismutase (Fe-SOD), Cu/Zn superoxide dismutase (Cu/Zn-SOD), and manganese superoxide dismutase (Mn-SOD), are distinguished. Under water deficit, the up-regulated expression of genes encoding the antioxidant enzymes both at the transcriptional and post-transcriptional level as well as the enhancement of enzyme activities, were observed (30, 31, 32).

Herein, we hypothesize that under water deficit in specific environmental conditions, especially those preventing the development of deep root system *F. arundinacea* and *F. glaucescens* could cope with this stress activating a set of similar survival strategies, involving mostly drought tolerance and recovery after stress cessation. We also assume that these strategies will be manifested at the levels of both photosynthetic performance and cellular antioxidant system. Thus, the comprehensive research presented in this paper involved (*i*) the analysis of gene expression at transcript and protein levels for the

selected enzymes of Calvin cycle (fructose-1,6-bisphosphate aldolase (pFBA), phosphoglycerate kinase (PGK) and glyceraldehyde-3-phosphate dehydrogenase (GAPDH)) and (*ii*) the activity of pFBA, as a protein marker of the Calvin cycle, (iii) the analysis of gene expression at protein level for the selected antioxidant enzymes (GR, GPX, APX, CAT, Fe-SOD, Cu/Zn-SOD, and Mn-SOD), (*iv*) the measurements of a set of physiological parameters precisely describing a plant's physiological status under control, drought and re-watering conditions. These parameters included a relative water content (RWC), electrolyte leakage (EL), lipid peroxidation, chlorophyll fluorescence, gas exchange, and level of ROS generations.

Results

Genomic structure of *F. arundinacea* and *F. glaucescens*

Allotetraploid *F. arundinacea* had 42 chromosomes, while tetraploid *F. glaucescens* had 28 chromosomes in total, respectively. Our results indicate that, the hybridization of 5S rDNA revealed six signals in chromosomes of the HDR and the LDR genotypes of *F. arundinacea* and four signals in both genotypes of *F. glaucescens* (Fig. 1, red signals). In all the analysed plants, 5S rDNA loci were located in the interstitial part of chromosomes. The results of fluorescent *in situ* hybridization (FISH) using 35S rDNA sequence as a probe showed the same number of signals in both genotypes of *F. arundinacea* and *F. glaucescens* (Fig. 1, green signals). However, these four signals were distributed in a different way in these two species. In *F. arundinacea* karyotypes, one pair of chromosomes with the terminal position of 35S rDNA and one pair with the interstitial position of this sequence (Fig. 1A and B), were observed. For both *F. glaucescens* genotypes, only the terminal distribution of 35S rDNA was noticed (Fig. 1C and D).

Phenotypic observations under drought and recovery

Under severe drought stage a leaf rolling phenomenon was noticeable in both genotypes of *F. arundinacea* and *F. glaucescens*. After rehydration, the leaves returned to their usual shape in all the analyzed genotypes, nevertheless numerous of dried leaves could be observed (Fig. 2). Both *F. glaucescens* genotypes had stronger growth inhibition during water deficit, compared with the *F. arundinacea* genotypes.

Physiological parameters

The significant drop of RWC was observed on the 11^{th} day (D3) of stress treatment comparing to the control conditions (value 95-98%) in all the analyzed genotypes. However, in the LDR genotypes of both *Festuca* species (Fa-LDR and Fg-LDR) RWC reduction was notably larger (value around 40%) than in both HDR genotypes (Fa-HDR and Fg-HDR) (value around 70%). After further re-watering RWC increased to the level similar to the control conditions in all genotypes. Both, in the control conditions, initial phase of

drought (D1, D2) and after stress cessation there were no significant differences in RWC dynamic between the *F. arundinacea* and *F. glaucescens* genotypes (Fig. 3A).

The values of EL did not change during the whole drought period in both HDR genotypes of both *Festuca* species but it significantly increased on the 11th day (D3) of water deficit in both LDR genotypes. Much higher EL growth was noted for the Fg-LDT genotype. However, after re-watering, the EL values decreased to the control level in both LDR genotypes (Fig. 3B).

In the severe drought (D3) both analyzed genotypes of *F. arundinacea* and *F. glaucescens* reduced significantly, to a similar level, their CO_2 assimilation rate (A), stomatal conductance (g_s) and transpiration (E) values. Interestingly, in the control conditions higher A and g_s were reported for the Fa-HDR genotype and the Fg-LDR genotype. After re-watering, CO_2 assimilation rate increased slightly but significantly only in the Fg-LDR genotype, while transpiration was higher in comparison to the drought conditions only in the Fa-LDR genotype (Fig. 4A, B and C). The intracellular concentration of CO_2 (Ci) increased significantly in all the genotypes during the stress treatment. After further re-watering, a reduction of this parameter was observed in all the genotypes, except the Fg-HDR genotype (Fig. 4D).

In the Fa-HDR genotype, the majority of parameters of chlorophyll fluorescence remained stable or decreased during prolonged drought. Values of the following parameters: ABS/RC, ABS/CS, TR0/RC and TR0/CS demonstrated significant differences between the Fa-HDR and Fa-LDR genotypes, but only at D3 time-point of drought stress. The ABS/RC, ABS/CS and TR0/RC increased significantly in the Fa-LDR genotype in the advanced drought (Fig. S1A, B, C). ET0/CS parameter declined notably, in both *F. arundinacea* genotypes and slightly increased after re-watering (Fig. S1E). No significant changes in all the analyzed fluorescence parameters between the Fa-LDR and Fa-HDR genotypes after stress cessation, were noticed (Fig. S1, Fig. S2). Significant differences between the Fg-HDR and Fg-LDR genotypes of *F. glaucescens* on the 11th day (D3) of drought were observed in numerous parameters (ET0/Cs, RC/CSm, DI0/RC, DI0/CS) (Fig. S1E, Fig. S2A, C, D). These changes were resulted from a decrease or increase in the values of these parameters in the Fg-LDR genotype at D3 time-point. After recovery, in the Fg-LDR genotype, all the changed parameters returned to values observed in the control conditions or in the initial phase of stress. In several measured parameters of chlorophyll fluorescence (ABC/RC, ET0/CS, RC/CSm, RC/CS0, DI0/RC) significant differences were visible between the Fg-HDR and Fg-LDR genotypes after drought cessation (Fig. S1A, E, Fig. S2A, B, C). These differences were mainly due to a reduction of the values observed in the Fg-HDR genotype and an increase in the Fg-LDR genotype. Only in case of ABS/RC, TR0/RC and DI0/RC, an increase was observed in the Fg-HDR genotype at RH time-point (Fig. S1A, C, Fig. S2C).

Expression of genes encoding the Calvin cycle enzymes at transcript and protein levels

The transcription profiles patterns of PGK and pFBA were similar in both *F. arundinacea* genotypes (Fa-HDR and Fa-LDR). After initial increase on the 3rd day of drought (D1), decrease to the control level was observed. No changes in transcript accumulation, comparing to the control in analyzed genotypes, were noticed after re-watering. However, clear differences between the genotypes (Fa-HDR and Fa-LDR) in PGK and pFBA transcript level were visible after re-watering (RH) and on the 3rd day of drought (D1), respectively. The control level of PGK transcript was equal in both *F. glaucescens* genotypes, whereas pFBA transcript accumulation was about twofold higher in the Fg-HDR than in Fg-LDR genotype. Under water deficit, transcript level of both PGK and pFBA significantly decreased in the Fg-HDR and Fg-LDR genotypes, achieving the lowest values on the 11th day of stress (D3). After rehydration PGK level was significantly higher comparing to the control in both genotypes, whereas pFBA level only in the Fg-LDR genotype. The clear differences under stress conditions between the *F. glaucescens* genotypes in PGK and pFBA transcript abundance were observed at D1 and D2, respectively (Fig. 5A, B).

GAPDH transcript level increased on the 11th day (D3) of water deficit, comparing to the control in both *F. arundinacea* genotypes and it was significantly higher in the Fa-HDR genotype. After stress cessation it returned to the initial level. In the HDR genotype of *F. glaucescens* GAPDH level remained relatively stable during whole drought period, however it increased about twofold after re-watering. In the Fg-LDR genotype a slight drop of transcript level was observed at D2 time-point. During the whole period of experiment the level of GAPDH was higher in the Fg-LDR genotype than in the Fg-HDR genotype (Fig. 5C).

A significant growth of PGK protein level at the beginning of stress duration (between D1-D2) was observed in the LDR genotype of *F. arundinacea.* In the advanced drought (D3) it decreased to the lower level than observed in the control conditions, while in the recovery phase it returned to the initial level. In the Fa-HDR genotype PGK protein level decreased in the late stage of stress (D2 and D3). The increase of accumulation level of PGK protein in both genotypes of *F. glauacescens* was observed during the first six days of drought duration. Then its level decreased on the 11th day (D3) of drought and increased back after stress cessation in both genotypes. However, only in Fg-HDR plants the accumulation exceeded the control (Fig. 6A).

No relevant changes in the pFBA accumulation level in the Fa-LDR genotype during the whole experiment, were observed. In the Fa-HDR genotype, a slight increase was noticed on the 3rd and 11th day of water deficit. However, that accumulation level dropped again after rehydration to the values observed in the control conditions. The accumulation level of pFBA protein in the Fg-HDR genotype increased from the initial time-points of drought duration (D1-D2) to the rehydration time-point (RH). Interestingly, its level was constant during the whole experiment in the Fg-LDR genotype (Fig. 6B).

The amount of GAPDH protein was more or less constant during drought treatment in two *F. arundinacea* genotypes, and it dropped after rehydration. The similar tendency was observed for *F. glaucescens* genotypes, however, after re-watering, the amount of GAPDH decreased only in the Fg-LDR genotype (Fig. 6C).

Chloroplast aldolase activity

The activity of pFBA decreased in both *F. arundinacea* genotypes in response to drought. In the Fa-HDR genotype lowered activity was observed during the whole stress period, whereas in the Fa-LDR genotype only on the 11th (D3) day of drought. In the recovery phase pFBA activity increased to the control level only in the Fa-LDR genotype. In *F. glaucescens* genotypes, a significant decline of pFBA activity was observed between the 6th (D2) and 11th (D3) day of drought, compared to the control. After re-watering an increase of pFBA activity comparing to the advanced water deficit (D3) was revealed for both *F. glaucescens* genotypes, but it was lower than in the control. The genotypes differed with pFBA activity during the whole stress period, that was higher in the Fg-HDR genotype (Fig. 7).

Expression of genes coding antioxidant enzymes at the protein level

The protein accumulation of Cu/Zn-SOD was rather stable during the whole experiment in both *Festuca* species. Its slight reduction in the initial phase of stress duration (D1) and higher accumulation, compared to control at D3, were observed in the Fa-HDR genotype and Fg-LDR genotypes, respectively. The lowering of its level was also noticeable in both *F. arundinacea* genotypes after re-hydration. In the control conditions the protein level of Mn-SOD was about twofold higher in the Fa-HDR genotype than in the Fa-LDR genotype. During the whole drought period, its level was elevated in the Fa-LDR, and then it dropped and returned to the control level after stress cessation (RH). In the Fa-HDR genotype, the reduced protein level of Mn-SOD in D2 and after re-watering, was noticed. A significant Mn-SOD accumulation was observed between the 6th and 11th day (D2-D3) of stress duration in the Fg-HDR genotype. In the Fg-LDR genotype a slow declined of Mn-SOD protein level was remarked during the whole experiment in relation to control. The slight increase of Fe-SOD protein amount was observed only at the beginning of stress treatment (D1) in the Fa-HDR genotype. In the Fa-LDR genotype, a significant reduction in the amount of Fe-SOD during water deficit, was observed. After re-watering it returned to the control level. In the Fg-LDR genotype the Fe-SOD protein was highly accumulated during the stress treatment as well as after regeneration (Fig. 8A, B, C).

Stress-induced changes in APX protein accumulation were noticed in the Fa-LDR genotype. The protein level was reduced comparing to the control during the whole drought period and after re-watering. Lowered APX protein level was also observed at D2 in the Fg-HDR genotype and at D2 and D3 time-points in the Fg-LDR genotype (Fig. 9A). In the Fa-HDR genotype a statistically significant decrease of GPX, was observed during the treatment (Fig. 9B, C). In contrary, in the Fg-HDR genotype, the accumulation level of the GPX was higher under stress treatment and after re-watering. In the Fg-LDR genotype a decrease at more advanced time-points of drought (D2, D3), was observed (Fig. 9B). On the 3rd day (D1) of water deficit a significant decrease of GR in the Fa-HDR genotype, was shown. This was the only time-point at which differences in GR amount between *F. arundinacea* genotypes, were revealed. On the other hand, the higher accumulation level of GR for the Fg-HDR, compared to the Fg-LDR genotype, was demonstrated during the whole experiment (Fig. 9C). No significant changes in CAT abundance during drought and after

rehydration was shown for the Fa-LDR genotype. In case of the Fa-HDR genotype, the amount of this protein was elevated at three time-points (D1, D3 and RH). Significant differences in the accumulation level of CAT between *F. glaucescens* genotypes were visible at all the experimental time-points, and their levels were always higher in case of the Fg-HDR genotype (Fig. 9D).

Lipid peroxidation

Under water deficit TBARS accumulation increased in both *F. arundinacea* genotypes. The initiall growth in D1 and then decrease in D2 was noticed in the Fa-LDR genotype. However, the highest *ca.* threefold grow of TBARS was observed on the 11^{th} day of drought (D3) in both genotypes of *F. arundinacea.* Furthermore, this elevated level of TRARS was stable after re-watering. In the Fg-HDR genotype, TBARS accumulation level showed a downward trend reaching the lowest level at D3. On the other hand, it increased significantly at D1 and D3 time-points in the Fg-LDR genotype, but dropped again, even below the level observed in the control conditions, after stress cessation (Fig. 10A).

Superoxide anion radical and hydrogen peroxide level

The amount of superoxide anion radical decreased drastically at the beginning of water deficit (D1), compared to the control in both *F. arundinacea* genotypes. However, in the subsequent day of stress its level started to rise. In the Fa-HDR genotype it reached the value observed in the control on the 11^{th} day of drought, whereas in the Fa-LDR genotype on the day 6^{th} and 11^{th} it remained lower than in the control. The content of $O_2^{\bullet -}$ did not change after re-watering in the Fa-HDR but increased more in the Fa-LDR plant. Contrary, in the *F. glaucescens* genotypes, a slight reduction of $O_2^{\bullet -}$ amount at the D1 and D2 time-points of water deficit was observed only for the Fg-LDR plants. In the advanced drought (D3) its content was significantly higher in both Fg-HDR and Fg-LDR genotypes, compared to control condition, however, without significant differences between the genotypes. Both *F. glaucescens* genotypes revealed diminished accumulation level of the molecule after stress cessation (Fig. 10B).

A significant reduction of hydrogen peroxide accumulation level between the control and the 6^{th} day (D2) of drought was reported for both *F. arundinacea* genotypes. At the D3 time-point this level was stable in the Fa-HDR genotype, whereas in the Fa-LDR its value significantly increased. A decrease of hydrogen peroxide accumulation level was observed for both *F. arundinacea* after stress cessation. The accumulation of H_2O_2 increased in the Fg-LDR genotype on the 11^{th} day (D3) of drought. However, at the beginning of stress treatment (D1, D2) its level slightly decreased in both genotypes of *F. glaucescens*. Furthermore, a significant reduction in H_2O_2 generation was noticed for the two genotypes but was more deeper for the Fg-LDR genotype, after stress treatment (RH) (Fig. 10C).

Discussion

The plants response to water deficiency is a combination of biological mechanisms that involve morphological, physiological and molecular adaptations. They use different strategies to survive under stress conditions that trigger several metabolic pathways at the same time (14). Acquired strategy of majority of the plant species strongly depends on the environmental conditions. Certainly, the efficient photosynthesis and the activation of enzymatic antioxidant system under drought are among important goals.

Our earlier research performed on *F. arundinacea* allowed to recognize crucial components of leaf metabolisms as well as roots performance, including its architecture and metabolism, involved in drought resistance of this species (5, 33). On the other hand, it has been here first time when general response to drought in *F. glaucescens* at the physiological as well as molecular levels was more deeply analysed. The species identities were confirmed by using FISH with rDNA probes. Both species presented the karyotypes precisely characterized earlier by Thomas et al. (1997) (34).

Physiological response to drought

The reduction of RWC could be a good indicator of cellular dehydration in plants, including grass species (5, 35). Our results clearly indicate that both genotypes of *F. arundinacea* and *F. glaucescens* were suffered from water deficit. However, the higher reduction of leaf RWC in the stress conditions were observed in both LDR genotypes, what could be partially due to differences in root metabolism and more efficient water uptake in case of HDR plants at the early stage of the stress (36). Our recent study proved that in case of *F. arundinacea*, deep root system is not sufficient to fully avoid cellular damage, caused by drought. In the experiment performed in tubes, thus enabling undisturbed development of root system, it was demonstrated that not only architecture but also metabolic performance of roots were crucial to cope with negative effect of water deficit by using different survival strategies (33).

The chlorophyll fluorescence parameters provides the information about the efficiency of flow of energy from antenna to the electron transport chain components through the reaction centre of photosystem II (PSII) (37). Photochemical processes were more affected in the Fa-LDR and Fg-LDR genotypes, compared to the HDR genotypes. However, both LDR genotypes showed a high capacity of regeneration after stress cessation, which resulted in a return to the levels similar to the control conditions. Interestingly, in the Fg-HDR genotype no significant changes during drought treatment were observed in numerous parameters, while their significant decrease after re-watering, was visible.

The physiological analysis clearly indicated that cellular response to water deficit was very similar in case of *F. arundinacea* and *F. glaucensens*, at least with respect to the analyzed parameters. Furthermore, the HDR plants of both species were able to avoid strong cellular dehydration and membrane damage at the advanced drought. On the other hand, the LDR plants of both species demonstrated a high capacity to regenerate their metabolism after stress cessation. The level of CO_2 assimilation under stress and control conditions was in case of both species dependent, at least partially, on stomata aperture.

The level of membrane integrity under drought and oxidative stress was recognized through the EL and MDA level measurements. The EL was the other physiological parameter, with similar dynamics in case of both species. It was unchanged in the HDR genotypes of both species during the whole experiment, whereas in both LDR genotypes, it was relatively high in the advanced drought conditions. However, after re-watering, it dropped to the control values. Observations for *F. arundinacea* genotypes correspond with our earlier results described by Kosmala et al. (2012) (5) and show that recovery after stress cessation is the strategy developed by both species. We demonstrated here that drought caused a lipid peroxidation in both genotypes of *F. arundinacea*, at the advanced (D3) and also at the initial stage of water deficit (D1) in the LDR. Furthermore, this parameter remained at the high level also after rehydration in both genotypes. The dynamics of lipid peroxidation in response to drought was similar only in the LDR genotype of *F. glaucescens*. Similarly to the EL, the MDA content in the Fg-HDR genotype only slightly decreased in the advanced drought. Interestingly, several studies indicated that the MDA level increased in green tissues of plants (citrus, maize) exposed to a combination of abiotic stresses, such as drought and heat (10 d, 40 °C). Furthermore, in a single stress application, the MDA did not increase or it was relatively low (38, 39, 40). On the other hand, higher than in the control, the level of MDA after re-watering in both *F. arundinacea* genotypes and in the LDR of *F. glaucescens* indicates a more efficient functioning of defense mechanisms in the first species. Moreover, the Fg-LDR genotypes of *F. glaucescens* was a highest capacity to regenerate damaged cellular membranes.

A reduction of gas exchange parameters observed at the D3 time-point (the 11^{th} day of water deficit), compared to the control conditions, was similar in *F. arundinacea* and *F. glaucescens*. On the other hand, the values of these parameters were maintained at lower levels also after 10 days of watering in both species. It shows that recovery period was not sufficient in both species to bring back optimal efficiency of photosynthesis. It indicates that stomatal regulation of photosynthesis dominates in both species. It was shown here, in the analyzed genotypes of both species, that stomata closure significantly limited CO_2 content. However, several earlier studies, including ours, indicated that the efficiency of the Calvin cycle could be also responsible for that phenomenon, as an important component of non-stomatal limitations of photosynthesis (8, 16, 41).

Efficiency of Calvin cycle

In the case of presented results in both *F. arundinacea* genotypes, elevated transcript level of pFBA and PGK genes was observed at the beginning of stress duration (D1). It was correlated with the protein accumulation of those enzymes but only in the Fa-HDR genotype. In *F. glaucescens*, drought conditions induced accumulation of PGK in both genotypes as well as pFBA in the Fg-HDR genotype. The elevated levels of PGK and pFBA in *F. glaucescens* were also observed during recovery phase in the more resistant genotype what was not noticeable in the Fg-LDR genotype. During recovery phase, the protein level of these two enzymes was the highest in the Fg-HDR genotype. We can assume that the PGK and pFBA are involved in more efficient dark phase of photosynthesis what acquires drought tolerance.

The up-regulation of GAPDH in *F. arundinacea* in the advanced drought, was noticed while in *F. glaucescens* drought did not significantly affect the relative expression level of this gene, which was higher in the Fg-LDR genotype.

Interestingly, the Fa-HDR and the Fg-HDR genotypes, accumulated higher amounts of pFBA protein during the whole period of water deficiency. This enzyme was shown to be crucial for the efficiency of the Calvin cycle under drought conditions in our earlier experiment performed on *L. multiflorum/F. arundinacea* introgression forms (8, 16). However, the higher abundance of pFBA during drought period was followed by its higher activity only in case of the Fg-HDR genotype. No clear and significant differences with respect to pFBA activity were revealed between analyzed here *F. arundinacea* genotypes. Thus, we can conclude that non-stomatal regulations of CO_2 assimilation under drought, with respect to pFBA accumulation and activity, were not crucial in case of *F. arundinacea*, and even in case of *F. glaucescens*. Net photosynthesis in relation to all the analyzed here genotypes fully followed the levels of stomatal conductance, despite the observed differences in pFBA abundance and activity between the *F. glaucescens* genotypes.

ROS production and performance of enzymatic antioxidant system

Reactive oxygen species are involved in plant development processes. The balance between their production and scavenging plays a crucial role in a proper functioning of plants. Abiotic stresses occurrence in the environment lead to elevated ROS generation that causes cellular damage (42). However, the increase of cellular antioxidant activity could enhance the protection against oxidative damage caused by stresses, including drought (43, 44, 45). Our results show that water deficit did not generate the high level of ROS favouring oxidative stress in the analyzed species. An initial decrease in superoxide anion radical and hydrogen peroxide release may be caused by effective functioning of antioxidant system in response to early water deficit. The prolongation of stress duration contributed to a generation of significantly higher amount of superoxide anion radical in both *F. glaucescens* genotypes. After further re-watering, the abundance of ROS dropped to levels in the control conditions or it was even lower.

The protein levels of Mn-SOD, APX, GPX, GR and CAT were significantly higher in the Fg-HDR genotype than in the Fg-LDR genotype. These results indicate that the Fg-HDR genotype exhibited higher antioxidant protein accumulation against ROS-induced oxidative stress damage than did the Fg-LDR genotype.

The superoxide dismutases with different metal co-factor are the enzymes that catalyze the dismutation of superoxide anion radical into molecular oxygen (O_2) or hydrogen peroxide (H_2O_2). In plant cells, Fe-SOD are located in chloroplasts, Mn-SOD in mitochondria and peroxisomes, and Cu/Zn-SOD in chloroplasts, cytosol, and possibly also in extracellular space (46). Accumulation of Fe-SOD and Mn-SOD in the Fg-LDR and Fg-HDR genotype, respectively may be associated with the compensatory mechanisms

to counteract enhanced superoxide anion radical production in the response to drought stress in *F. glaucescens*.

Noteworthily, $O_2^{\cdot-}$ amount raised 2.5-fold in succulent purslane under heat and combined stress, but not in plants exposed to drought (40). In cotton cultivars, no significant differences in H_2O_2 levels were observed for drought and combined drought/heat stress (42). It is well known that catalase, which is involved in the degradation of H_2O_2 into water and oxygen, is the major H_2O_2-scavenging enzyme in plants (47). In our analyses, we observed a decline of H_2O_2 level throughout the experiment in the Fa-HDR genotype. We infer that this result might be due to the increase of catalase accumulation during water deficit. Furthermore, a significantly lower generation of H_2O_2 in the Fg-HDR genotype, compared to the Fg-LDR genotype, was correlated with the higher accumulation level of CAT.

Interestingly, the elevated level of TBARS in both genotypes of *F. arundinacea* at D1, D3 and RH time-points were not correlated with a higher level of H_2O_2 and superoxide anion radical. These results imply that in *F. arundinacea* and *F. glaucescens* other factors, including other ROS, contributed to the observed lipid peroxidation. Moreover, a lipoxygenase-dependent lipid peroxidation can occur to form lipid hydroperoxides (48) used e.g. as substrates for drought-induced jasmonic acid synthesis. It should be noted that the maintenance of low or moderate level of ROS during stress can facilitate their function as second messengers mediating defense/tolerance reactions in plant cells, including stomatal closure or programmed cell death (49).

Conclusions

Our analyses clearly shows that physiological reactions to water deficit were similar in both HDR and LDR genotypes of *Festuca* species. The HDR genotypes were able to maintain water homeostasis and membrane stability during stress treatment, whereas the LDR genotypes revealed higher recovery capacity after stress cessation. This clearly shows that physiological reaction to drought was similar in both species. However, *F. arundinacea* and *F. glaucescens* revealed significant differences in the potential to tolerate tissue dehydration what was correlated with a distinct expression level of the Calvin cycle enzymes under stress. It was showed that in *F. glaucescens* PGK and pFBA expression was involved in both dehydration tolerance and recovery. Moreover, maintenance of stable efficiency of dark phase of photosynthesis seems to be crucial for drought tolerance and recovery in *F. glaucescnes*. On the other hand, the acquisition of drought tolerance (tissue dehydration) in *F. arundinacea* and *F. glaucescens* does not involve marked changes at the protein level in the enzymatic antioxidant system. Presented results clearly indicated that in case of pot-experimental conditions both species were characterized by a similar drought response mainly consisting of drought tolerance and recovery that was clearly indicated at the physiological level. All performed analysis were presented in the scheme (Fig. 11) which summarized the similarities and differences between all tested genotypes during water deficit as well as after re-hydration.

Methods

Plant material, growth conditions and experimental design

For the analysis, two genotypes within each species, *F. arundinacea* cv. Kord (2n = 6x = 42) and *F. glaucescens* (*F. arundinacea* Schreb. subsp. *Fenas* (Lag.) *Arcang*.) (2n = 4x = 28), significantly differing with the potential of drought resistance: high drought resistant (HDR) and low drought resistant (LDR), were used (Tab. 1). The drought resistance of the selected genotypes was evaluated based on the measurements of chlorophyll fluorescence (OJIP) during short-term drought treatment (11-day water deficit and further 10-day recovery) performed on the pot-planted plants growing in the environmental chamber (hereafter termed pot-experiment) (5). The genotypes of *F. arundinacea* derived from single seeds originated from the collection of Institute of Plant Genetics, Polish Academy of Sciences, created by prof. Zbigniew Zwierzykowski. The seeds of *F. glaucescens* (ABY-Bn 354-1980) derived from the collection of the Institute of Biological, Environmental and Rural Sciences (IBERS) (UK), originated from the Centre de Recherches de Lusignan, INRA (France) and donated in 1985 to IBERS. This collection at IBERS was hold by the Genetic Resources Unit (Mr Ian D., Thomas). The analysis of genomic structure was performed for both species, *F. arundinacea* and *F. glaucescens*, to precisely confirm their identity.

The genotypes of both *Festuca* species were exposed for short-term drought in the pot-experiment as described previously by Kosmala et al. (2012) (5). Each genotype was represented by 15 independent clones (each three growing in a separate pot with 4 dm^3 of sand : peat (1:3) mixture). The conditions of experiment were as follows: temperature – 22 °C, 16 h photoperiod, 400 µmol $m^{-2}s^{-1}$ PPFD (photosynthetic photon flux density), air humidity 50-60%. Plant material (leaf tissue) for the analysis was harvested before stress treatment when plants were fully hydrated (control, C), on the 3rd (D1), 6th (D2) and 11th (D3) day of watering cessation, and 10 days after subsequent re-watering (RH) (Fig. 12).

Fluorescent *in situ* hybridization (FISH) analysis

To verify the genomic status of *F. arundinacea* and *F. glaucescens* plants, FISH experiment with two highly conserved rDNA sequences (5S and 35S rDNA) as probes was applied. The wheat clone pTa794 containing 5S rDNA was labeled by PCR with tetramethyl-rhodamine-5-dUTP (Roche, Mannheim, Germany). Whereas, 35S rDNA, generated from a 2.3 kb fragment of the 25S rDNA coding region of *Arabidopsis thaliana*, was labeled by nick-translation with digoxigenin-11-dUTP (Roche, Mannheim, Germany). The preparation of slides, the labeling of probes and FISH experiments were performed according to protocols described in Majka et al. (2017) (50). Briefly, in FISH protocol, a hybridization mixture consisted of 50% formamide, 2 × SSC, 10% dextran sulfate and 100 ng of rDNA probes. The hybridization mixture together with the good quality of chromosome slides were denatured at 80 °C for 2 min and then incubated overnight at 37 °C. In the protocol, it was applied fluorescein isothiocyanate-conjugated (FITC) anti-digoxigenin antibody to detect digoxigenin-labeled 35S rDNA probe. After counterstaining with 4, 6-diamidino-2-phenylindole (DAPI, Sigma, St. Louis, Missouri), the slides were mounted in antifade Vectashield solution (Vector Laboratories, Burlingame, CA, USA). Slides were evaluated under an Olympus BX 61 automatic epifluorescence microscope equipped with an Olympus

XM10 CCD camera. All images were captured using Olympus Cell-F imaging software (ver. 3.1; Olympus Soft Imaging Solutions GmbH, Germany) and Micrographx Picture Publisher software (ver. 10; Corel Corporation, Canada).

Physiological parameters

A relative water content (RWC), electrolyte leakage (EL), chlorophyll ‘a’ fluorescence and gas exchange (net photosynthesis (CO_2 assimilation), transpiration, stomatal conductance) were measured as described previously in detail by Kosmala et al. (2012) and Perlikowski et al. (2014) (5, 8). For all the physiological measurements, the second fully expanded leaves from the top of the plant were used. The RWC was calculated according to the following formula: RWC% = (FW-DW)/(SW-DW)×100, where FW was the leaf fresh weight, DW was the leaf dry weight, and SW was the leaf turgid weight. The EL was measured using conductivity meter (Hanna Instruments EC215 Conductivity Meter) and calculated as follows: L1/L2 X 100, where L1 and L2 were electrolyte leakage of the fresh leaves and the leaves frozen in liquid nitrogen, respectively. Chlorophyll ‘a’ fluorescence was measured by the HandyPEA fluorimeter (Hansatech Instruments Ltd., King's Lynn, England) during midday. For RWC, EL, and chlorophyll ‘a’ fluorescence measurements three biological and ten technical replicates of all the analyzed genotypes at each time-points of experiment (C, D1, D2, D3, RH), were applied. Gas exchange was measured through CIRAS-2 Portable Photosynthesis System (PP SYSTEMS) at three selected time-points (C, D3, and RH) in three biological replicates.

Transcript levels of Calvin cycle enzymes under drought and recovery

RT-qPCR analyses were carried out for chloroplastic fructose-1,6-bisphosphate aldolase (pFBA), phosphoglycerate kinase (PGK) and glyceraldehyde-3-phosphate dehydrogenase (GAPDH). Total RNA was extracted from 100 mg of the leaves using the RNeasy Plant Mini Kit (Qiagen) according to the protocol. The remaining DNA was removed from the samples using the RNase-Free DNase set (Qiagen). The cDNA was synthesized with the Maxima First Strand cDNA Synthesis Kit (Thermo Scientific). The RT-qPCR assays were performed using the FastStart Essential DNA Probes Master (Roche) through the Bio-Rad CFX 96 thermal system as described by Pawłowicz et al. (2018) (7). The reaction temperature profile was as follows: initial denaturation 95 °C for 10 min, followed by 44 cycles of 95 °C for 10 s, and 60 °C for 30 s and final 50 °C for 30 s. The relative quantification method (ΔΔCq) was used. The reactions were normalized using actin and ubiquitin as reference genes. The expression stability of reference genes under drought conditions was evaluated using the BestKeeper software. Primers and TaqMan probes of analyzed genes were designed through the Beacon Designer software. All the measurements were carried out in three biological and two technical replicates.

Protein levels of Calvin cycle enzymes and antioxidant enzymes under drought and recovery

Protein accumulation profiles of three enzymes of Calvin cycle (pFBA, PGK, GAPDH) and seven antioxidant enzymes including: glutathione reductase (GR, AS06 181), chloroplastic glutathione peroxidase (GPX, AS04 055), chloroplastic Fe-dependent superoxide dismutase (FeSOD, AS06 125), chloroplastic Cu/Zn superoxide dismutase (Cu/Zn-SOD, AS06 170), manganese superoxide dismutase (Mn-SOD, AS09 524), L-ascorbate peroxidase (APX, AS08 368) and catalase (CAT, AS09 501), were analyzed. Total proteins were extracted from the leaves using Hurkman and Tanaka protocol with slight modifications (4, 51, 52). Briefly, the 200 mg of powdered tissue was homogenized with 500 µl of extraction buffer (0.7 M sucrose, 0.5 M TRIS, 30 mM HCl, 50 mM EDTA, 2% DTT, and 0.1 M KCl). An equal volume of phenol was then added, vortexed and centrifuged at 21 500 g for 15 min. The upper phenol phase was transferred to new tubes and 500 µl of extraction buffer was added. After vortexing and centrifuging in the same conditions, the proteins from the phenol phase were precipitated by the addition of 5 volumes of cold 0.1 M ammonium acetate in methanol in the new tube. After at least overnight incubation at -20 °C, the samples were centrifuged at 9 000 g at 0 °C for 30 min. The precipitate was washed once with the cold ammonium acetate in methanol and twice in cold acetone, and dried in SpeedVac (Heraeus Instruments). Dried precipitate was dissolved in 150 µl of resolving buffer (50 mM TRIS, 2% SDS, DTT) at room temperature (RT) and then denatured for 5 minutes at 99 °C. Western blot assay was performed as described by Pawłowicz et al. (2012) (53). Briefly, proteins were separated by 12% SDS-polyacrylamide gel and electroblotted (Trans-blot SD, Semi-Dry Transfer Cell, Bio-Rad) onto nitrocellulose membranes (Bio-Rad). Immunodetections of pFBA, PGK and GAPDH were performed with the use of polyclonal antibodies (Agrisera) diluted at 1:4000. The protein level of antioxidant enzymes was detected using the commercial rabbit polyclonal antibodies (Agrisera). The GR, GPX, Fe-SOD, Cu/Zn-SOD, MnSOD, and CAT antibodies were diluted at 1:4000, whereas the APX antibody was diluted at 1:2000. The membranes were incubated with the antibodies for 1 h. Antigen–antibody complexes were detected using a secondary anti-rabbit IgG–horse radish peroxidase conjugate (Sigma) in dilution 1:20000 (1 h of incubation), chemiluminescent substrates Westar Supernova (Cyanogen) and ChemiDoc^{TM}Touch Igmagin System (Bio-Rad) to visualize the results.

Chloroplast aldolase activity under drought and recovery

The activity of pFBA in the leaves was measured according to the modified method of Sibley-Lehninger (54, 55). Chloroplast proteins were extracted as described by Kosmala et al. (2012) and Perlikowski et al. (2016) with slight modifications (5, 8). The amount of 1 g of frozen material was ground in a liquid nitrogen and then suspended in 10 ml of chloroplast isolation buffer (CIB) (Sigma) with 0,1% BSA. The homogenised samples were filtered through a Sefar nitrex filter and centrifuged at 200 g at RT for 3 min. The collected supernatant was subsequently centrifuged for 15 min at 900 g at RT and then washed two times in 4 ml of CIB solution. Each time, the suspension was centrifuged at 900 g at RT for 15 min. The chloroplast pellet was dissolved in 500 µl of 0.1 M phosphate buffer (0.1 M Na_2HPO_4) with 3% Triton X100, shaken by vortex and centrifuged at 21 500 g in RT for 10 min. The collected supernatant was used to determine the pFBA activity. The volume of 100 µl 0.06 M fructose-1,6-bisphosphate and 140 µl of incubation buffer (0.05 M 2,4,6-trimethylpyridine, 0.08 M hydrazine sulfate, 0.3 mM sodium iodoacetate)

pH 7.4 was pre-incubated in water bath for 10 min at 30 °C. Additionally, a material sample was performed for each biological replication which contained 100 µl of 0.06 M fructose-1,6-bisphosphate, 140 µl of incubation buffer and 300 µl of 10% trichloroacetic acid (TCA). The volume of 20 µl of chloroplast extract was added to the pre-incubated solutions, mixed and incubated at 30 °C for 45 min. The reaction was stopped by adding 300 µl of 10% TCA to the solution, and tubes were chilled on ice. Ice-chilled samples were centrifuged at 21 500 g for 10 min in RT to remove the precipitated proteins. The volume of 100 µl of each supernatant was incubated with 100 µl of 0.75 M NaOH at RT for 10 min and after that 100 µl of 0.1% 2,4-dinitrophenylhydrasine was added and the samples were incubated for 10 minutes in a water bath at 30 °C. The tubes were taken out and 700 µl of 0.75 M NaOH was added to them and mixed well. After 3 min of incubation, the absorbance at 540 nm was measured against the material sample. A standard curve was prepared with use of 0.01 mM D-glyceraldehyde as described in Perlikowski et al. (2016) (8). The amount of produced trioses in the pFBA assay was read according to the standard curve and after calculations of glyceraldehyde mg produced by 1 g of plant sample during 1 h.

Lipid peroxidation under drought and recovery (TBARS assay)

The level of lipid peroxidation was measured spectrophotometrically as a content in the samples of the thiobarbituric-reactive substances (TBARS) according to the method of Heath and Packer (1968) with slight modifications (56, 57, 58). Briefly, 300 mg of fresh leaves were homogenized with 2 ml of a buffer containing 0.25% TBA in 10% TCA at RT. After homogenization, samples were incubated at 100 °C for 15 min in a water bath. Next, the samples were cooled on ice and centrifuged at 10 000 g by 10 min at 4 °C. The supernatant was collected and the absorbance was measured at λ = 532 nm and at λ = 600. Amount of TBARS was calculated through the following formula: TBARS (µM) = $(A_{532} – A_{600})/155$, where 155 was an extinction factor.

Superoxide anion radical and hydrogen peroxide under drought and recovery

The level of superoxide anion radical ($O_2^{\bullet -}$) and hydrogen peroxide (H_2O_2), were assayed spectrophotometrically. Superoxide anion radical measurement was performed according to Doke (1983), and Arasimowicz et al. (2009) (59, 60). Nitroblue tetrazolium (NBT) was used as a substrate which undergoes reduction by $O_2^{\bullet -}$ to form diformazan. Leaf discs (0.6-0.8 cm in diameter) were incubated with 3 ml of mixture containing 0.05 M potassium-phosphate buffer (pH 7.8) with 0.1 mM EDTA, 10 mM NaN_3 and 0.05% NBT, for 1 h in the dark. Next, the samples were heated at 85 °C by 15 min and cooled down on ice. The absorbance was measured at λ = 580 nm. The level of $O_2^{\bullet -}$ was expressed as absorbance at 580 nm per 1 g of fresh weight (FW).

The concentration of hydrogen peroxide (H_2O_2) was assayed using the titanium ($Ti4^+$) method (61, 62). The amount of 400 mg of plant tissue was homogenized on ice with 1.5 ml of 0.1 M potassium-phosphate buffer, pH 7.8. Obtained extracts were centrifuged at 14 000 g at 4 °C by 25 min. The volume of 1.5 ml of reaction mixture containing 400 µl of enzymatic extract, 600 µl of potassium-phosphate buffer and 500 µl of titanium reagent (0.6 mM PRL and 0.6 mM PTO in a ratio 1:1) were prepared for each samples. After 10 min of incubation, the absorbance was measured at λ = 508 nm. The standard curve was used. The level of H_2O_2 was determined on the basis of absorbance and expressed as µmol H_2O_2 per 1 g of fresh weight (FW).

Statistical analysis

All the statistical analyses were performed with the STATISTICA 10.0 software (StatSoft, Tulsa OK, USA). A two-way analyses of variance (ANOVA), with genotype and time-point as classification factors, were performed. Differences in physiological parameters, protein accumulation, pFBA activity, RT-qPCR, TBARS assay, ROS measurement between the plants during experiment duration were evaluated using Fisher's least significant difference (LSD) test at P = 0.01. Homogeneity groups according to test were denoted by the same letters on the graphs.

Abbreviations

ABS/CS	energy flux for absorbed energy/CS
ABS/RC	energy flux for absorbed energy/RC
APX	L-ascorbate peroxidase
BSA	bovine serum albumin
CAT	catalase
Ci	internal CO2 concentration
CO2	carbon dioxide
CS	cross section of the leaf tissue
Cu/Zn-SOD	chloroplastic Cu/Zn superoxide dismutase
DI0/CS	energy flux for dissipated energy/CS
DI0/RC	energy flux for dissipated energy/RC
DTT	DL-dithiothreitol

DW	leaf dry weight
EDTA	ethylenediaminetetraacetic acid
EL	electrolyte leakage
ET0/CS	electron transport flux per CS
Fe-SOD	Fe-dependent superoxide dismutase
FISH	Fluorescent in situ hybridization
FW	Fe-dependent superoxide dismutase
GAPDH	glyceraldehyde-3-phosphate dehydrogenase
gs	stomatal conductance
GPX	glutathione peroxidase
GR	glutathione reductase
HDR	high drought tolerant
L1	electrical conductivity of the fresh leaf
L2	electrical conductivity of the leaf immersed in liquid nitrogen
LDR	low drought tolerant (LDR)
Mn-SOD	manganese superoxide dismutase
SDS	sodium dodecyl sulfate
SOD	superoxide dismutase
pFBA	fructose-1,6-bisphosphate aldolase
PGK	phosphoglycerate kinase
PPFD	photosynthetic photon flux density
PRL	4-(2'-pyridylazo)-resorcinol
PSII	photosystem II
PTO	potassium sodium tartrate tetrahydrate

RC	reaction center
RC/CS0	densities of active PSII at t = 0/CS
RC/CSm	densities of active PSII reaction centers at tmax (time to reach maximum fluorescence)
ROS	reactive oxygen species
RWC	relative water content
TBARS	the thiobarbituric-reactive substances
TR0/CS	energy flux for trapped energy/CS
TR0/RC	energy flux for trapped energy/RC

Supplementary Information

Additional files 1: Figure S1. Chlorophyll fluorescence measurments: ABS/RC (A), ABS/CS (B), TR0/RC (C), TR0/CS (D) and ET0/CS (E) in two genotypes of *F. arundinacea* (Fa-HDR, Fa-LDR) and *F. glaucescens* (Fg-HDR, Fg-LDR) before stress treatment (C), on the 3rd (D1), 6th (D2) and 11th (D3) day of water deficit and 10 days after re-hydration initiation (RH). The data represent means for ten individual measurements, error bars represent the standard errors (SE). Homogeneity groups according to Fischer LSD test (P = 0.01) are denoted by the same letters.

Additional files 2: Figure S2. Chlorophyll fluorescence measurments: RC/CSm (A), RC/CS0 (B), DI0/RC (C), DI0/CS (D) in two genotypes of *F. arundinacea* (Fa-HDR, Fa-LDR) and *F. glaucescens* (Fg-HDR, Fg-LDR) before stress treatment (C), on the 3rd (D1), 6th (D2) and 11th (D3) day of water deficit and 10 days after re-hydration initiation (RH). The data represent means for ten individual measurements, error bars represent the standard errors (SE). Homogeneity groups according to Fischer LSD test (P = 0.01) are denoted by the same letters.

Declarations

Ethics approval and consent to participate

Not applicable.

Consent for publication

Not applicable.

Availability of data and materials

Not applicable.

Competing interests

The authors declare that they have no competing interests.

Funding:

The research was supported by the National Science Centre (project no. 2016/23/B/NZ9/00820). Funding bodies were not involved in the design of the study and collection, analysis, interpretation of data and in writing the manuscript.

Authors' contributions

AK, MA-J conceived the ideas and designed the experiment. KL, IP, DP, AA and JM performed the experiments. KL performed the data analysis, KL and IP made a data interpretation. KL and JM prepared the figures and table. DP made statistics analysis. KL and IP wrote the article. AK and MA-J checked the manuscript.

Acknowledgements

We thank the Institute of Biological, Environmental and Rural Sciences (IBERS) (UK) for the seeds of *Festuca glaucescens*.

References

1. Gray SB, Brady SM. Plant developmental responses to climate change. Developmental Biology. 2016;419:64–7765.
2. Marshall AH, Collins RP, Humphreys MW, Scullion J. A new emphasis on root traits for perennial grass and legume varieties with environmental and ecological benefits. Food Energy Secur. 2016;5(1):26–39.
3. Augustyniak A, Perlikowski D, Rapacz M, Kościelniak J, Kosmala A. Insight into cellular proteome of *Lolium multiflorum/Festuca arundinacea* introgression forms to decipher crucial mechanisms of cold acclimation in forage grasses. Plant Sci. 2018;272:22–31.
4. Kosmala A, Bocian A, Rapacz M, Jurczyk B, Zwierzykowski Z. Identification of leaf proteins differentially accumulated during cold acclimation between *Festuca pratensis* plants with distinct levels of frost tolerance. J Exp Bot. 2009;60:3595–

5. Kosmala A, Perlikowski D, Pawłowicz I, Rapacz M. Changes in the chloroplast proteome following water deficit and subsequent watering in a high and a low drought tolerant genotype of *Festuca arundinacea*. J Exp Bot. 2012;63:6161–
6. Pawłowicz I, Rapacz M, Perlikowski D, Gondek K, Kosmala A. Abiotic stresses influence the transcript abundance of PIP and TIP aquaporins in *Festuca* J Appl Genet. 2017;58(4):421–435.
7. Pawłowicz I, Waśkiewicz A, Perlikowski D, Rapacz M, Ratajczak D, Kosmala A. Remodeling of chloroplast proteome under salinity affects salt tolerance of *Festuca arundinacea*. Photosynth Res. 2018;137:475–
8. Perlikowski D, Czyżniejewski M, Marczak Ł, Augustyniak A, Kosmala A. Water deficit affects primary metabolism differently in two *Lolium multiflorum/Festuca arundinacea* introgression forms with a distinct capacity for photosynthesis and membrane regeneration. Front Plant Sci. 2016;7:1063.
9. Perlikowski D, Augustyniak A, Masajada K, Skirycz A, Soja AM, Michaelis Ä, Wolter G, Kosmala A. Structural and metabolic alterations in root systems under limited water conditions in forage grasses of *Lolium-Festuca* complex. Plant Sci. 2019;283:211–223.
10. Humphreys MW, Thomas HM, Morgan WG, Meredith MR, Harper JA, Thomas H, Zwierzykowski Z, Ghesquière M. Discriminating the ancestral progenitors of hexaploid *Festuca arundinacea* using genomic *in situ* Heredity. 1995;75:171–174.
11. Thomas H, Humphreys MO. Progress and potential of interspecific hybrids of *Lolium* and *Festuca*. J Agric Sci. 1991;117:1–8.
12. Humphreys MW, Thomas HM, Harper J, Morgan G, James A, Ghamari-Zare A, Thomas H. Dissecting drought-and cold-tolerance traits in the *Lolium-Festuca* complex by introgression mapping. New Phytol. 1997;137:55–
13. Humphreys J, Harper JA, Armstead IP, Humphreys MW. Introgression-mapping of genes for drought resistance transferred from *Festuca arundinacea glaucescens* into *Lolium multiflorum*. Theor Appl Genet. 2005;110:579–587.
14. Fang Y, Xiong L. General mechanisms of drought response and their application in drought resistance improvement in plants. Cell Mol Life Sci. 2015;72:673–689.
15. Reddy AR, Chaitanya KV, Vivekanandan M. Drought-induced responses of photosynthesis and antioxidant metabolism in higher plants. J Plant Physiol. 2004;161:1189–1202.
16. Perlikowski D, Kosmala A, Rapacz M, Kościelniak J, Pawłowicz I, Zwierzykowski Z. Influence of short-term drought conditions and subsequent re-watering on the physiology and proteome of *Lolium multiflorum/Festuca arundinacea* introgression forms with contrasting levels of tolerance to long-term drought. Plant Biol. 2014;16:385–394.
17. Gill SS, Tuteja N. Reactive oxygen species and antioxidant machinery in abiotic stress tolerance in crop plants. Plant Physil Bioch. 2010;48:909–
18. Hossain MA, Bhattacharjee S, Armin SM, Qian P, Xin W, Li HY, Tran LSP. Hydrogen peroxide priming modulates abiotic oxidative stress tolerance: insights from ROS detoxification and scavenging. Front Plant Sci. 2015;6:420.

19. Miller G, Suzuki N, Ciftci-Yilmaz S, Mittler R. Reactive oxygen species homeostasis and signalling during drought and salinity stresses. Plan Cell and Environ. 2010;33:453–467.
20. Baxter A, Mittler R, Suzuki N. ROS as key players in plant stress signaling. J Exp Bot. 2014;65:1229–1240.
21. You J, Chan Z. ROS Regulation during abiotic stress responses in crop plants. Front Plant Sci. 2015;6:092.
22. Sofo A, Dichio B, Xiloyannis C, Masia A. Effects of different irradiance levels on some antioxidant enzymes and on malondialdehyde content during rewatering in olive tree. Plant Sci. 2004;166:293–
23. Campo S, Baldrich P, Messeguer J, Lalanne E, Coca M, San Segundo B. Overexpression of a calcium-dependent protein kinase confers salt and drought tolerance in rice by preventing membrane lipid peroxidation. Plant Physiol. 2014;165:688–704.
24. Gharibi S, Tabatabaei BE; Saeidi SG, Goli SAH. Effect of drought stress on total phenolic, lipid peroxidation, and antioxidant activity of *Achillea* Appl Biochem Biotech. 2016;178:796–809.
25. Cruz de Carvalho MH. Drought stress and reactive oxygen species: Production, scavenging and signalling. Plant Signal Behav. 2008;3:156–165.
26. Dubey AK, Kumar N, Kumar A, Ansari MA, Ranjan R, Gautam A, Meenakshi, Sahu N, Pandey V, Behera SK, Mallick S, Pande V, Sanyal I. Over-expression of CarMT gene modulates the physiological performance and antioxidant defense system to provide tolerance against drought stress in *Arabidopsis thaliana* Ecotoxicol Environ Saf. 2019;171:54–65.
27. Iqbal N, Hussain S, Raza MA, Yang CQ, Safdar ME, Brestic M, Aziz A, Hayyat MS, Asghar MA, Wang XC, Zhang J, Yang W, Liu J. Drought Tolerance of Soybean (*Glycine max* Merr.) by Improved Photosynthetic Characteristics and an Efficient Antioxidant Enzyme Activities Under a Split-Root System. Front Physiol. 2019;10:786.
28. Mittler R, Vanderauwera S, Gollery M, Van Breusegem F. Reactive oxygen gene network of plants.Trends Plant Sci. 2004;9:490–
29. Bailey-Serres J, Mittler R. The roles of reactive oxygen species in plant cells. Plant Physiol. 2006;141(2):311.
30. Laxa M, Liebthal M, Telman W, Chibani K, Dietz K-J. The Role of the Plant Antioxidant System in Drought Tolerance. Antioxidants. 2019;8:94.
31. Zhang C, Shi S, Liu Z, Yang F, Yin G. Drought tolerance in alfalfa (*Medicago sativa*) varieties is associated with enhanced antioxidative protection and declined lipid peroxidation. J Plant Physiol. 2019;232:226–240.
32. Luna CM, Pastori GM, Driscoll S, Groten K, Bernard S, Foyer CH. Drought controls on H_2O_2 accumulation, catalase (CAT) activity and CAT gene expression in wheat. J Exp Bot. 2005;56:417–423.
33. Perlikowski D, Augustyniak A, Skirycz A, Pawłowicz I, Masajada K, Michaelis Ä, Wolter G, Kosmala A. Efficient root metabolism improves drought resistance of *Festuca arundinacea*. Plant Cell Physiol.

2019;in print. DOI: 10.1093/pcp/pcz215.

34. Thomas HM, Harper JA, Meredith MR, Morgan WG, King IP. Physical mapping of ribosomal DNA sites in *Festuca arundinacea* and related species by *in situ* Genome. 1997;40:406–410.
35. Rampino P, Pataleo S, Gerardi C, Mita, G, Perrotta C. Drought stress response in wheat: physiological and molecular analysis of resistant and sensitive genotypes. Plant Cell Environ. 2006;29:2143–2152.
36. Wasson AP, Richards RA, Chatrath R, Misra SC, Sai Prasad SV, Rebetzke GJ, Kirkegaard JA, Christopher J, Watt M. Traits and selection strategies to improve root systems and water uptake in water-limited wheat crops. J Exp Bot. 2012;63(9)3485–3498.
37. Maxwell K, Johnson GN. Chlorophyll fluorescence – a practical guide. J Exp Bot. 2000;51:659–668.
38. Zandalinas SI, Balfagón D, Arbona V, Gómez-Cadenas A, Inupakutika MA, Mittler R. ABA is required for the accumulation of APX1 and MBF1c during a combination of water deficit and heat stress. J Exp Bot. 2016;67:5381–5390.
39. Zhao F, Zhang D, Zhao Y, Wang W, Yang H, Tai F, Li C, Hu X. The difference of physiological and proteomic changes in maize leaves adaptation to drought, heat, and combined both stresses. Front Plant Sci. 2016;7:1471.
40. Jin R, Wang Y, Liu R, Gou J, Chan Z. Physiological and metabolic changes of purslane (*Portulaca oleracea*) in response to drought, heat, and combined stresses. Front Plant Sci. 2016;6:1123.
41. Lawlor DW, Cornic G. Photosynthetic carbon assimilation and associated metabolism in relation to water deficits in higher plants. Plant Cell Environ. 2002;25:275–294.
42. Choudhury FK, Rivero RM, Blumwald E, Mittler R. Reactive oxygen species, abiotic stress and stress combination. Plant J. 2017;90:856–867.
43. Avramova V, AbdElgawad H, Vasileva I, Petrova AS, Holek A, Mariën J, Asard H, Beemster GTS. High Antioxidant Activity Facilitates Maintenance of Cell Division in Leaves of Drought Tolerant Maize Hybrids. Front Plant Sci. 2017;8:84.
44. Sheoran S, Thakur V, Narwal S, Turan R, Mamrutha HM, Singh V, Tiwari V, Sharma I. Differential Activity and Expression Profile of Antioxidant Enzymes and Physiological Changes in Wheat (*Triticum aestivum*) Under Drought. Appl Biochem Biotech. 2015;177(6):1282–1298.
45. Harb A, Awad D, Samarah N. Gene expression and activity of antioxidant enzymes in barley (*Hordeum vulgare*) under controlled severe drought. Plant-Environment Interactions. 2015;10(1):109–116.
46. Alscher RG, Erturk N, Heath LS. Role of superoxide dismutases (SODs) in controlling oxidative stress in plants. J Exp Bot. 2002;53(372):1331–1341.
47. Mhamdi A, Queval G, Chaouch S, Vanderauwera S, Van Breusegem F, Noctor G, Catalase function in plants: a focus on *Arabidopsis* mutants as stress-mimic models. J Exp Bot. 2010;61(15):4197–4220.
48. Alché JD. A concise appraisal of lipid oxidation and lipoxidation in higher plants. Redox Biol. 2019;7:101136.

49. Xie X, He Z, Chen N, Tang Z, Wang Q, Cai Y. The Roles of Environmental Factors in Regulation of Oxidative Stress in Plant. Biomed Res Int. 2019;9732325.
50. Majka J, Książczyk T, Kiełbowicz-Matuk A, Kopecký D, Kosmala A. Exploiting repetitive sequences and BAC clones in *Festuca pratensis* PLOS ONE. 2017;12(6):e0179043.
51. Hurkman WJ, Tanaka CK. Solubilization of plant membrane proteins for analysis by two-dimensional gel electrophoresis. Plant Physiol. 1986;81:802–806.
52. Masojć P, Kosmala A, Perlikowski D. Proteomic analysis of developing rye grain with contrasting resistance to preharvest sprouting. J Appl Genetics. 2013;54:11–19.
53. Pawłowicz I, Kosmala A, Rapacz M. Expression pattern of the psbO gene and its involvement in acclimation of the photosynthetic apparatus during abiotic stresses in *Festuca arundinacea* and *pratensis*. Acta Physiol Plant. 2012;34:1915–1924.
54. Sibley JA, Lehninger AL. Determination of aldolase in animal tissues. J Biol Chem. 1949;177:859–872.
55. Willard JM, Gibbs M. Role of aldolase in photosynthesis. II demonstration of aldolase types in photosynthetic organisms. Plant Physiol. 1968;43:793–798.
56. Heath RL, Packer L. Photoperoxidation in isolated chloroplasts. I. Kinetics and stoichiometry of fatty acid peroxidation. Arch Biochem Biophys. 1968;125:180–198.
57. Yagi K. Assay for serum lipid peroxide level its clinical significance. In: Yagi K, editors. Lipid peroxides in biology and medicine. London, New York: Academic Press Inc.; 1982. p. 223–241.
58. Arasimowicz-Jelonek M, Floryszak-Wieczorek J, Kosmala A. Are nitric oxide donors a valuable tool to study the functional role of nitric oxide in plant metabolism? Plant Biol. 2011;13:747–756.
59. Doke N. Involvement of superoxide anion generation in the hypersensitive response of potato tuber tissues to infection with an incompatible race of *Phytophthora infestans* and to the hyphal wall components. Physiol Plant Pathol. 1983;23:345–
60. Arasimowicz M, Floryszak-Wieczorek J, Milczarek G, Jelonek T. Nitric oxide, induced by wounding, mediates redox regulation in pelargonium leaves. Plant Biol. 2009;11:650–663.
61. Becana M, Aparicio-Tejo P, Irigoyen JJ, Sanchez-Diaz M. Some enzymes of hydrogen peroxide metabolism in leaves and root nodules of *Medicago sativa*. Plant Physiol. 1986;82:1169–1171.
62. Arasimowicz-Jelonek M, Floryszak-Wieczorek J, Gzyl J, Chmielowska-Bąk J. Homocysteine over-accumulation as the effect of potato leaves exposure to biotic stress. Plant Physiol Bioch. 2013;63:177–184.

Table

Table 1 Abbreviations of *F. arundinacea* and *F. glaucescens* genotypes used in the analyses and their definitions.

F. arundinacea	Fa-HDR	high drought resistant
	Fa-LDR	low drought resistant
F. glaucescens	Fg-HDR	high drought resistant
	Fg-LDR	low drought resistant

Figures

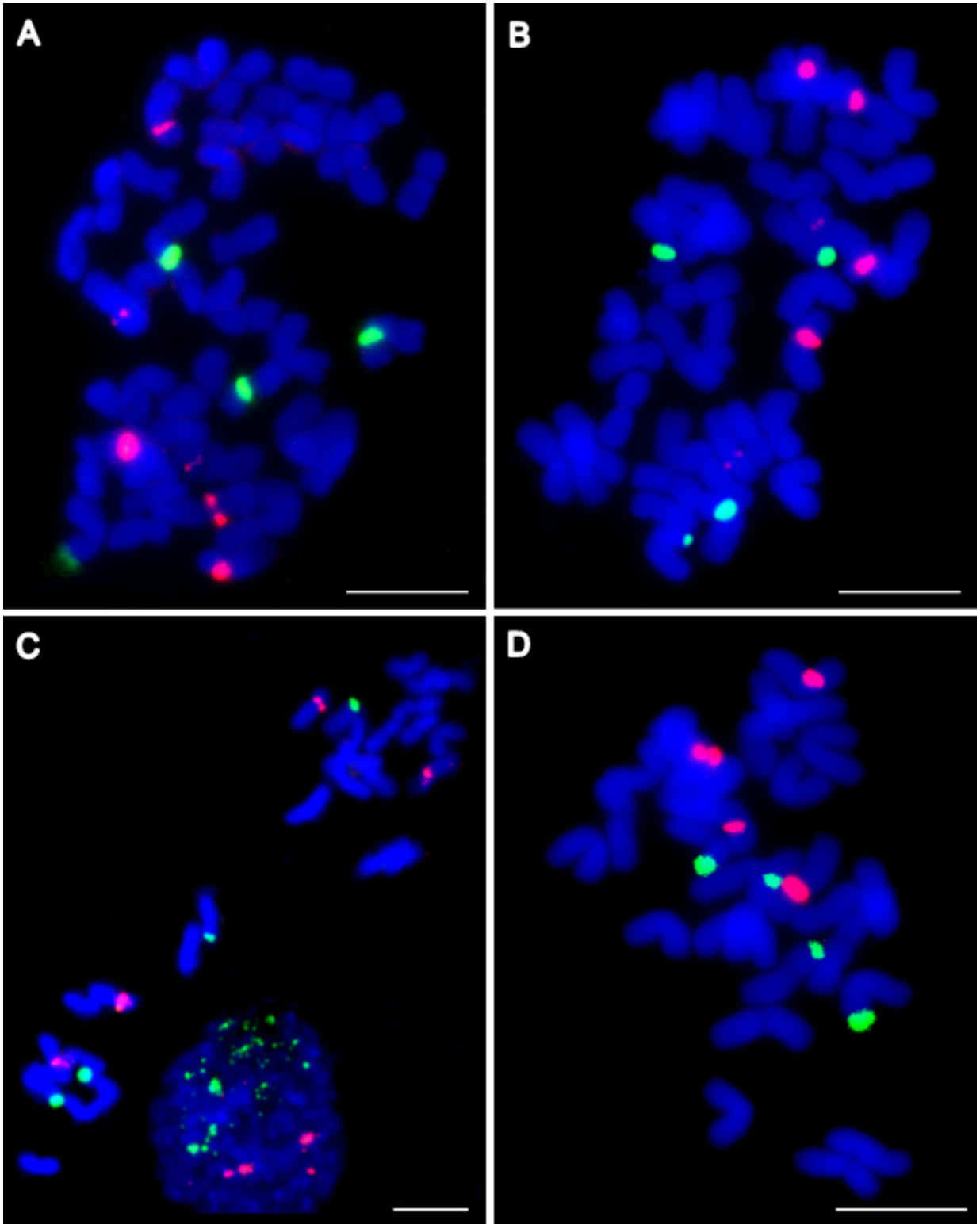

Figure 1

Distribution of rDNA sequences in metaphase chromosomes of F. arundinacea (2n = 6x = 42) and F. glaucescens (2n = 4x = 28). Fa-HDR genotype of F. arundinacea (A); Fa-LDR genotype of F. arundinacea (B); Fg-HDR genotype of F. glaucescens (C); Fg-LDR genotype of F. glaucescens (D). 5S rDNA - red; 35S rDNA - green; chromosomes counterstained with DAPI - blue. Scale bars 5 μm.

Figure 2

F. arundinacea and F. glaucescens in the control conditions, on the 11th day of drought (D3) and after re-watering (RH).

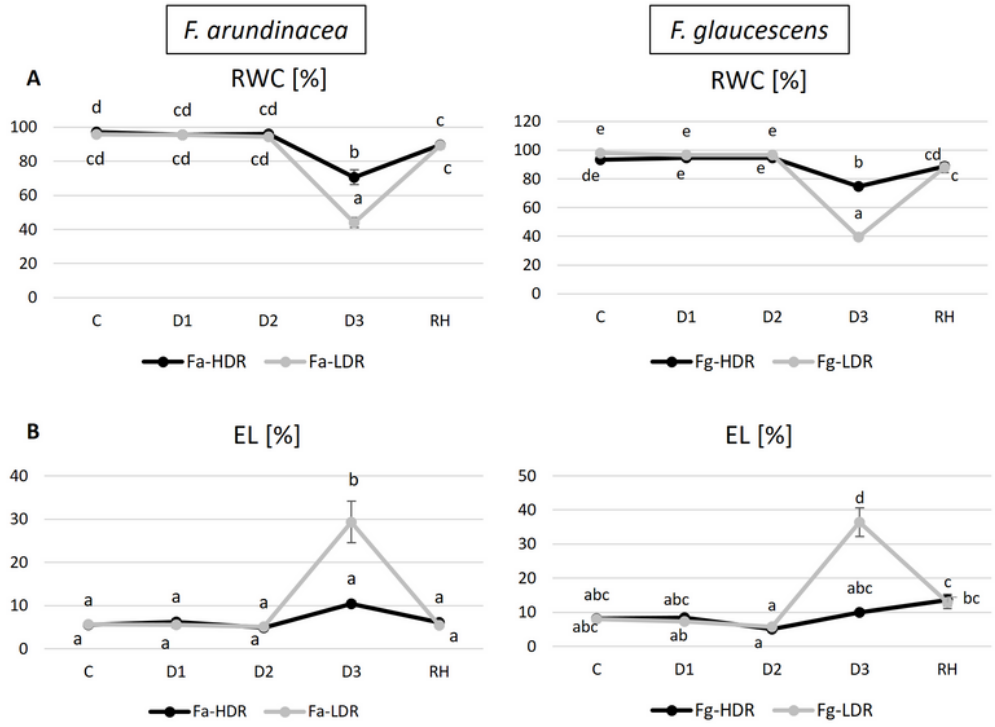

Figure 3

The relative water content (RWC) (A) and the electrolyte leakage (EL) (B) in two genotypes of F. arundinacea (Fa-HDR, Fa-LDR) and F. glaucescens (Fg-HDR, Fg-LDR) before stress treatment (C), on the 3rd (D1), 6th (D2) and 11th (D3) day of water deficit and 10 days after re-hydration initiation (RH). Error bars represent the standard errors (SE). Homogeneity groups according to Fischer LSD test (P = 0.01) are denoted by the same letters.

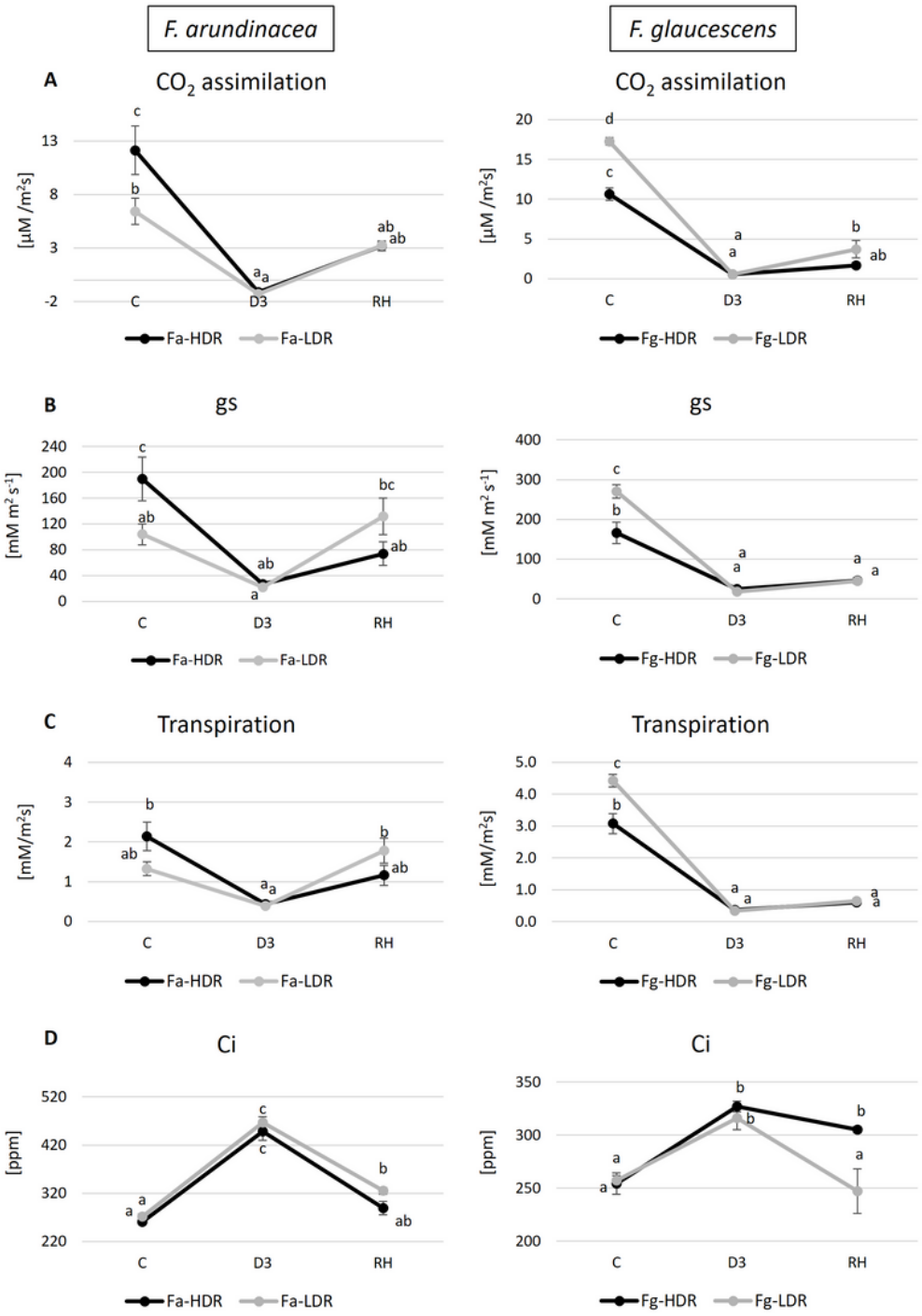

Figure 4

The gas exchange parameters (CO2 assimilation (A), stomatal conductance (gs) (B), transpiration (C), concentration of CO2 (Ci) (D)) in two genotypes of F. arundinacea (Fa-HDR, Fa-LDR) and F. glaucescens (Fg-HDR, Fg-LDR) before stress treatment (C), on 11th (D3) day of water deficit and 10 days after re-hydration initiation (RH). Error bars represent the standard errors (SE). Homogeneity groups according to Fischer LSD test (P = 0.01) are denoted by the same letters.

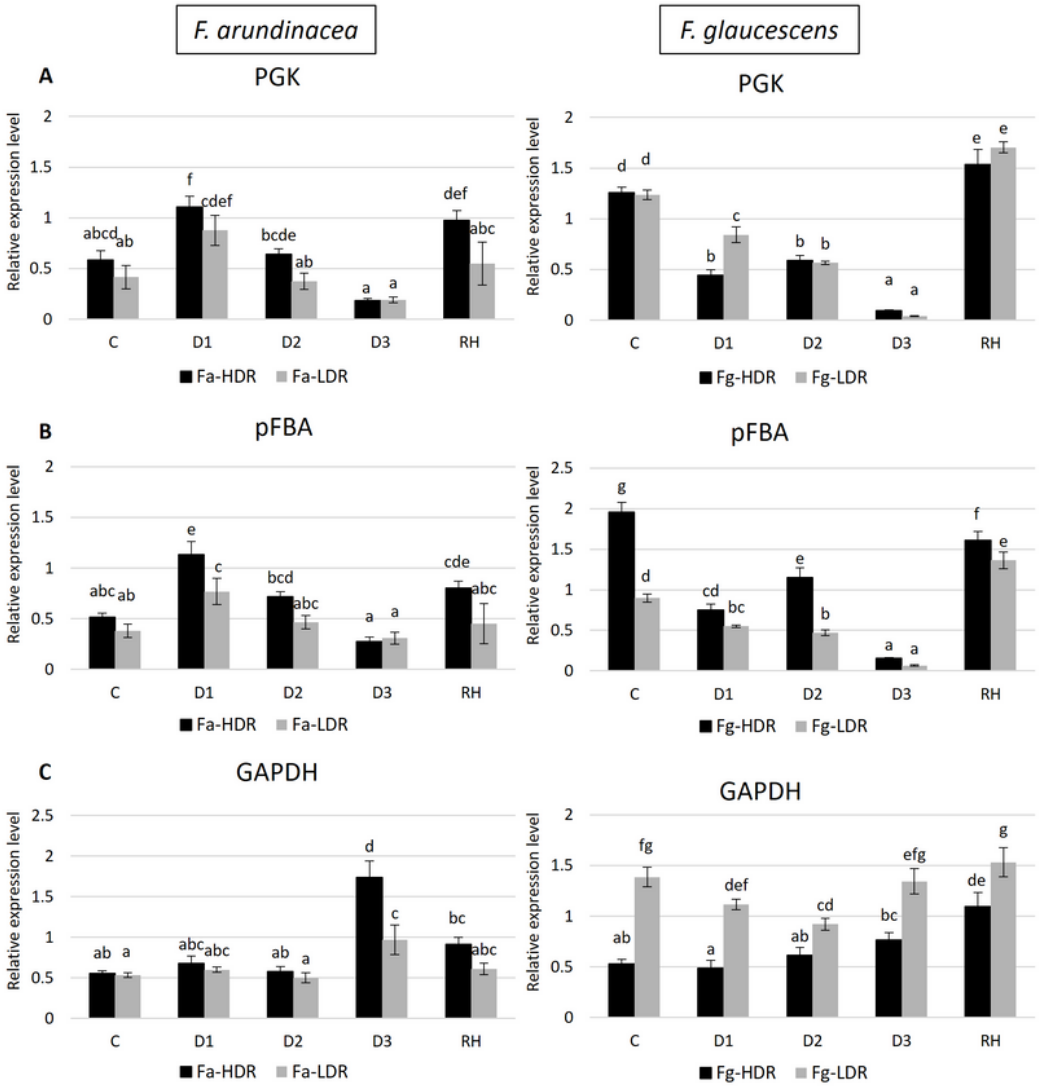

Figure 5

Relative expression level of phosphoglycerate kinase (PGK) (A), fructose-1,6-bisphosphate aldolase (pFBA) (B), and glyceraldehyde-3-phosphate dehydrogenase (GAPDH) (C) in two genotypes of F. arundinacea (Fa-HDR, Fa-LDR) and F. glaucescens (Fg-HDR, Fg-LDR) before stress treatment (C), on the 3rd (D1), 6th (D2) and 11th (D3) day of water deficit and 10 days after subsequent re-watering (RH). The transcript levels of actin and ubiquitin were used as references. Error bars represent the standard errors (SE) of three biological and two technical replicates. Homogeneity groups according to Fischer LSD test (P = 0.01) are denoted by the same letters.

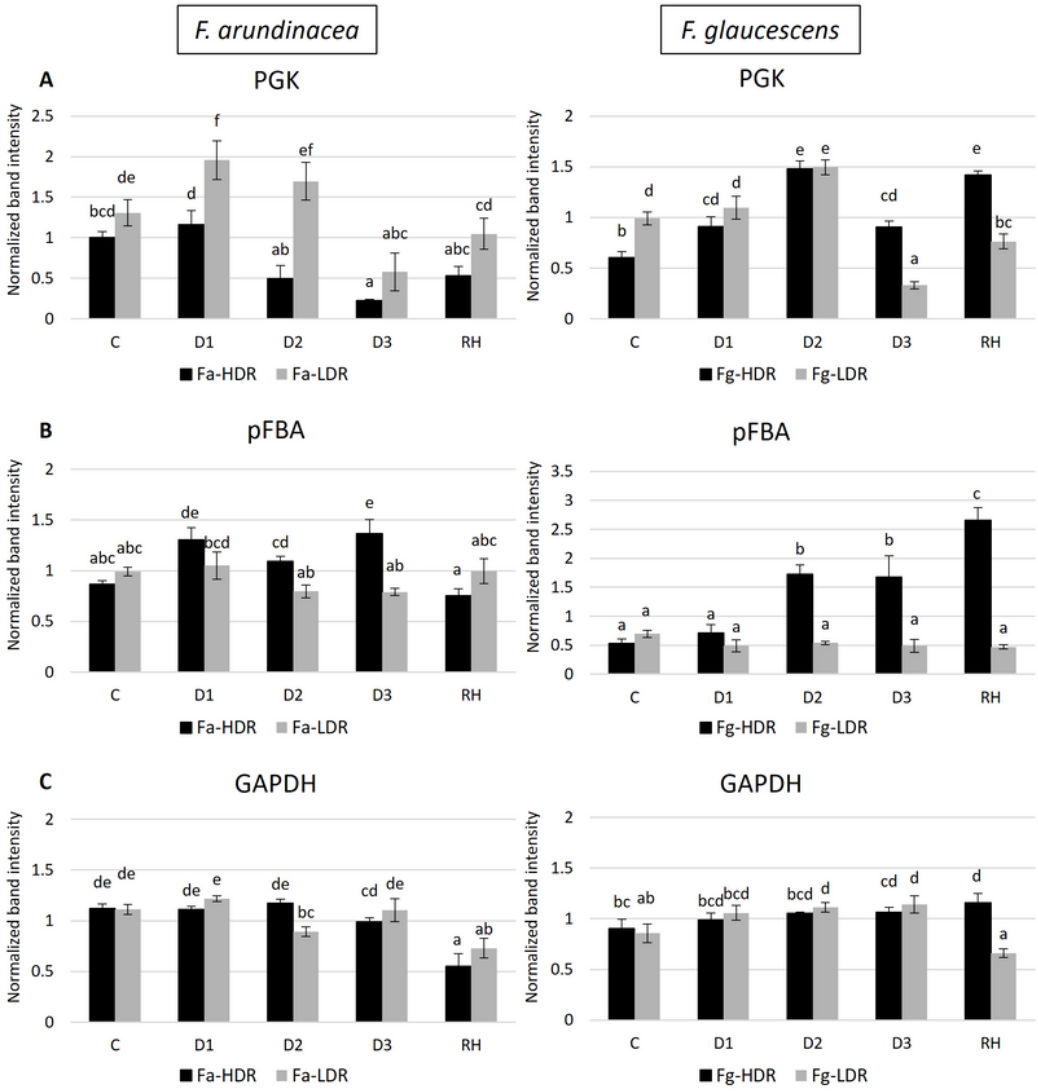

Figure 6

Protein level of phosphoglycerate kinase (PGK) (A), fructose-1,6-bisphosphate aldolase (pFBA) (B), and glyceraldehyde-3-phosphate dehydrogenase (GAPDH) (C) in two genotypes of F. arundinacea (Fa-HDR, Fa-LDR) and F. glaucescens (Fg-HDR, Fg-LDR) before stress treatment (C), on the 3rd (D1), 6th (D2) and 11th (D3) day of water deficit and 10 days after subsequent re-watering (RH). Error bars represent the standard errors (SE) of three biological and two technical replicates. Homogeneity groups according to Fischer LSD test (P = 0.01) are denoted by the same letters.

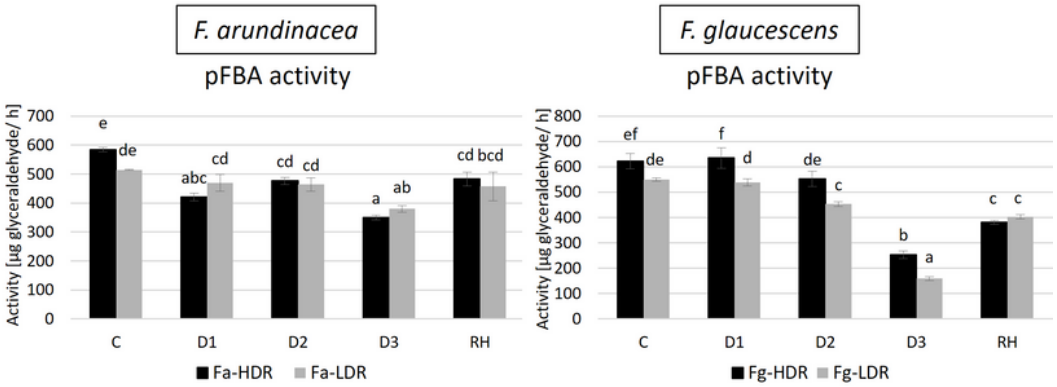

Figure 7

The activity of fructose-1,6-bisphosphate aldolase (pFBA) in two genotypes of F. arundinacea (Fa-HDR, Fa-LDR) and F. glaucescens (Fg-HDR, Fg-LDR) before stress treatment (C), on the 3rd (D1), 6th (D2) and 11th (D3) day of water deficit and 10 days after subsequent re-watering (RH). Error bars represent the standard errors (SE) of three biological and two technical replicates. Homogeneity groups according to Fischer LSD test (P = 0.01) are denoted by the same letters.

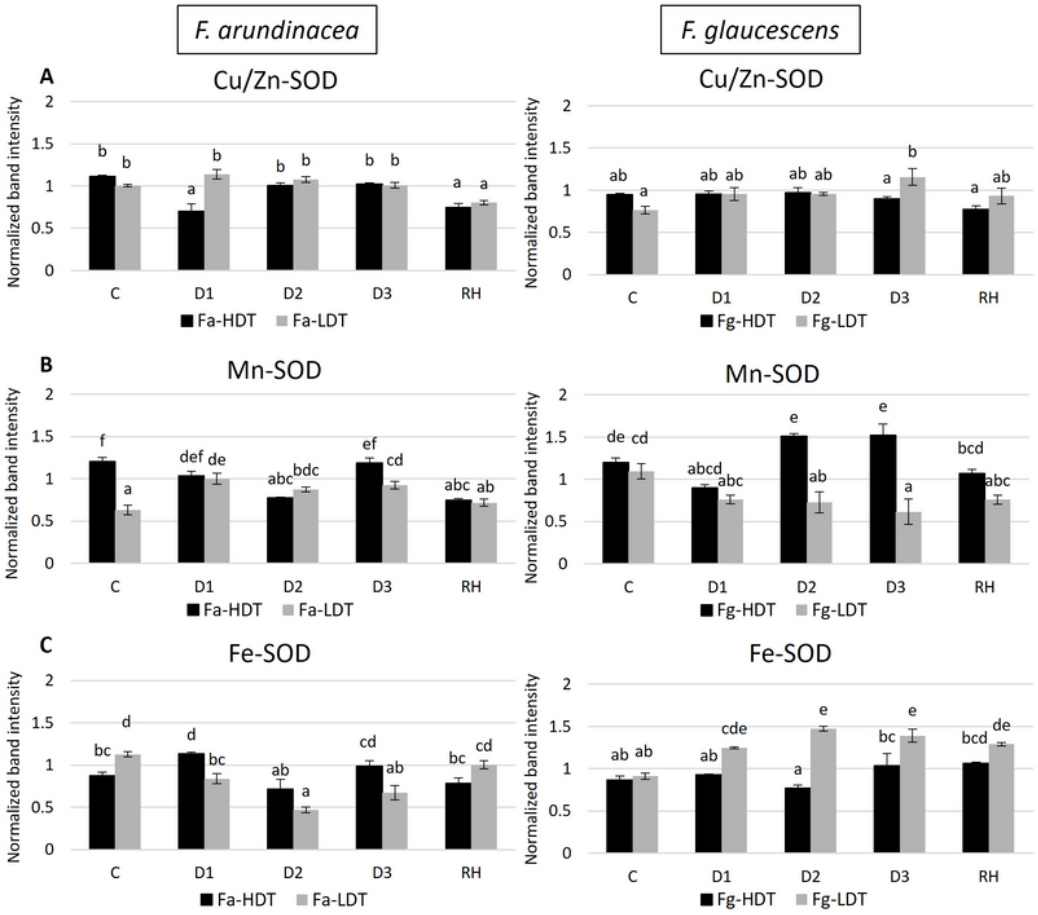

Figure 8

The protein level of Cu/Zn superoxide dismutase (Cu/Zn-SOD) (A), manganese superoxide dismutase (Mn-SOD) (B), Fe-dependent superoxide dismutase (Fe-SOD) (C) in two genotypes of F. arundinacea (Fa-HDR, Fa-LDR) and F. glaucescens (Fg-HDR, Fg-LDR) before stress treatment (C), on the 3rd (D1), 6th (D2) and 11th (D3) day of water deficit and 10 days after subsequent re-watering (RH). Error bars represent the standard errors (SE) of three biological and two technical replicates. Homogeneity groups according to Fischer LSD test (P = 0.01) are denoted by the same letters.

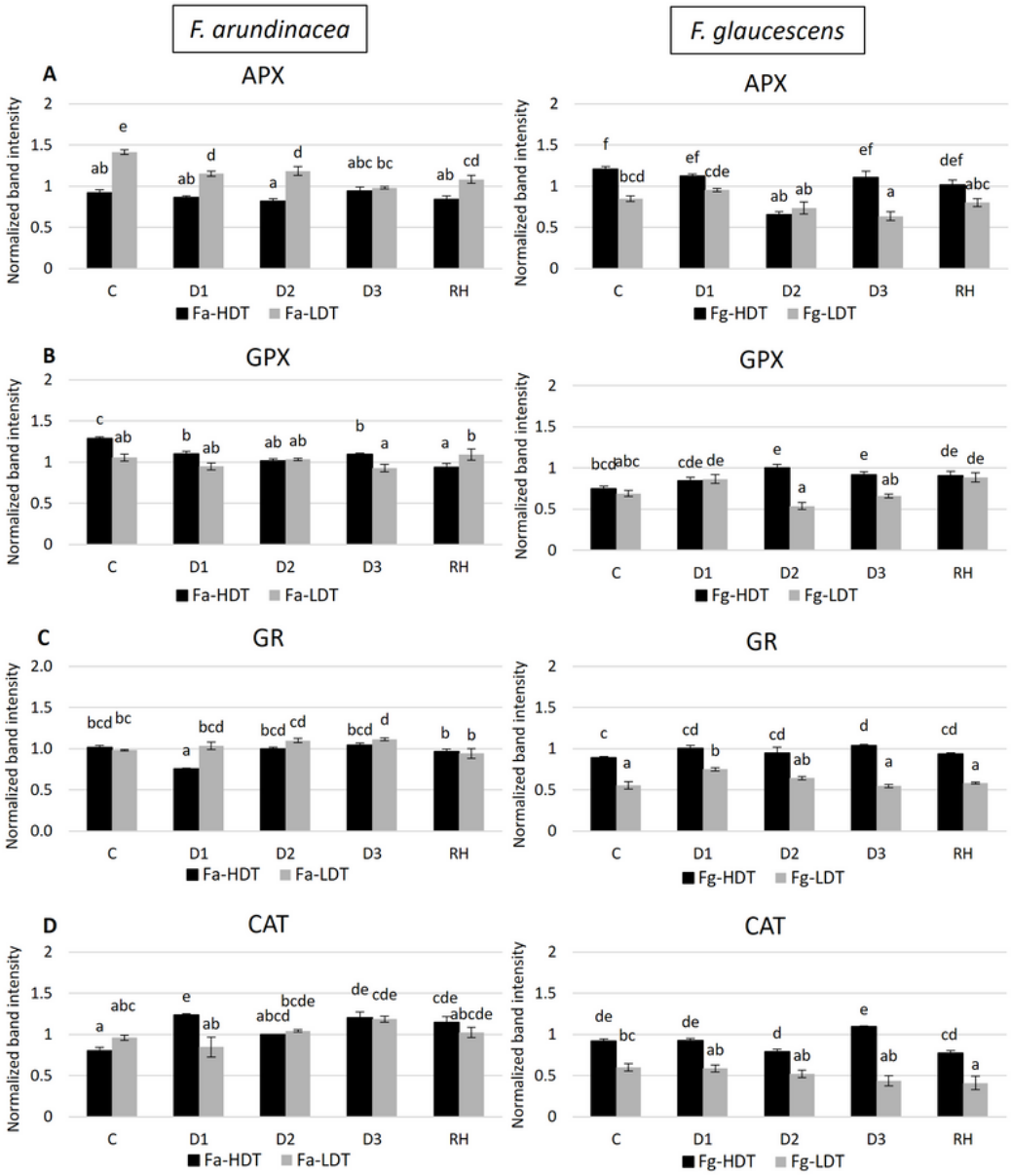

Figure 9

The protein level of L-ascorbate peroxidase (APX) (A), chloroplastic glutathione peroxidase (GPX) (B), glutathione reductase (GR) (C) and catalase (CAT) (D) in two genotypes of F. arundinacea (Fa-HDR, Fa-LDR) and F. glaucescens (Fg-HDR, Fg-LDR) before stress treatment (C), on the 3rd (D1), 6th (D2) and 11th (D3) day of water deficit and 10 days after subsequent re-watering (RH). Error bars represent the standard errors (SE) of three biological and two technical replicates. Homogeneity groups according to Fischer LSD test (P = 0.01) are denoted by the same letters.

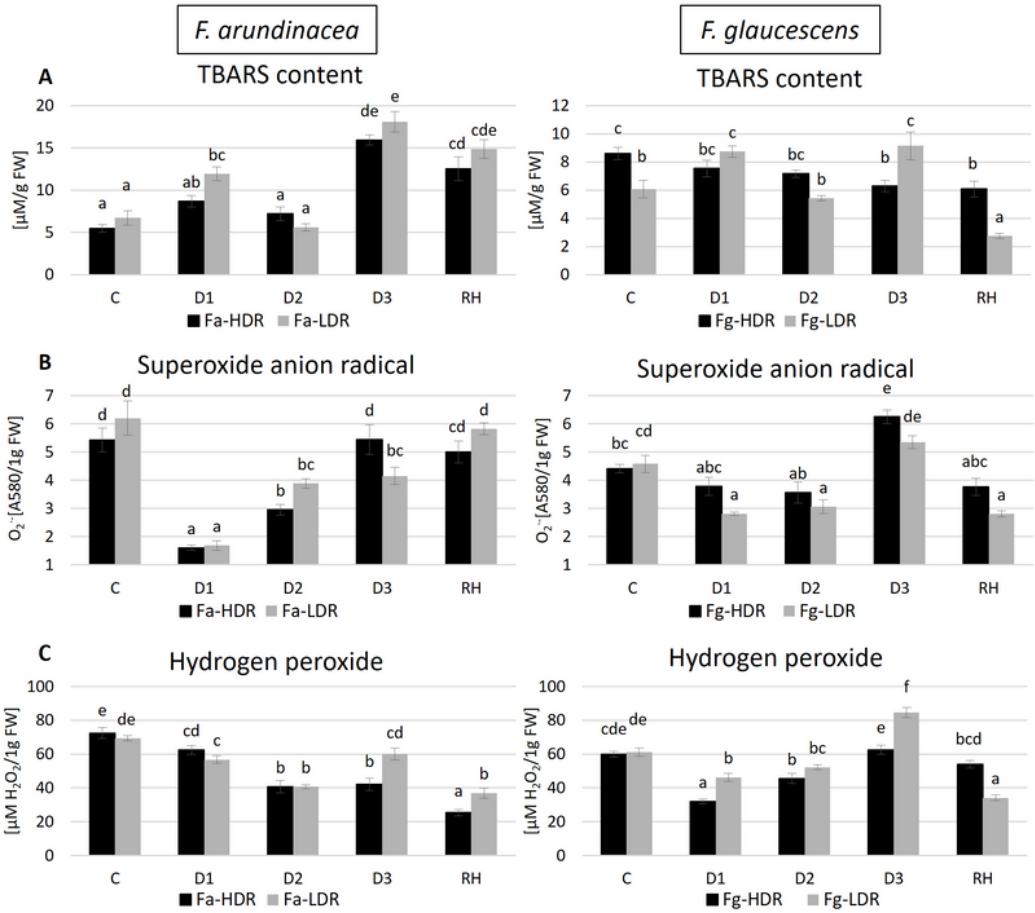

Figure 10

TBARS content (A), superoxide anion radical content (O2•−) (B), hydrogen peroxide content (H2O2) (C) in two genotypes of F. arundinacea (Fa-HDR, Fa-LDR) and F. glaucescens (Fg-HDR, Fg-LDR) before stress treatment (C), on the 3rd (D1), 6th (D2) and 11th (D3) day of water deficit and 10 days after subsequent re-watering (RH). Error bars represent the standard errors (SE) of three biological and two technical replicates. Homogeneity groups according to Fischer LSD test (P = 0.01) are denoted by the same letters.

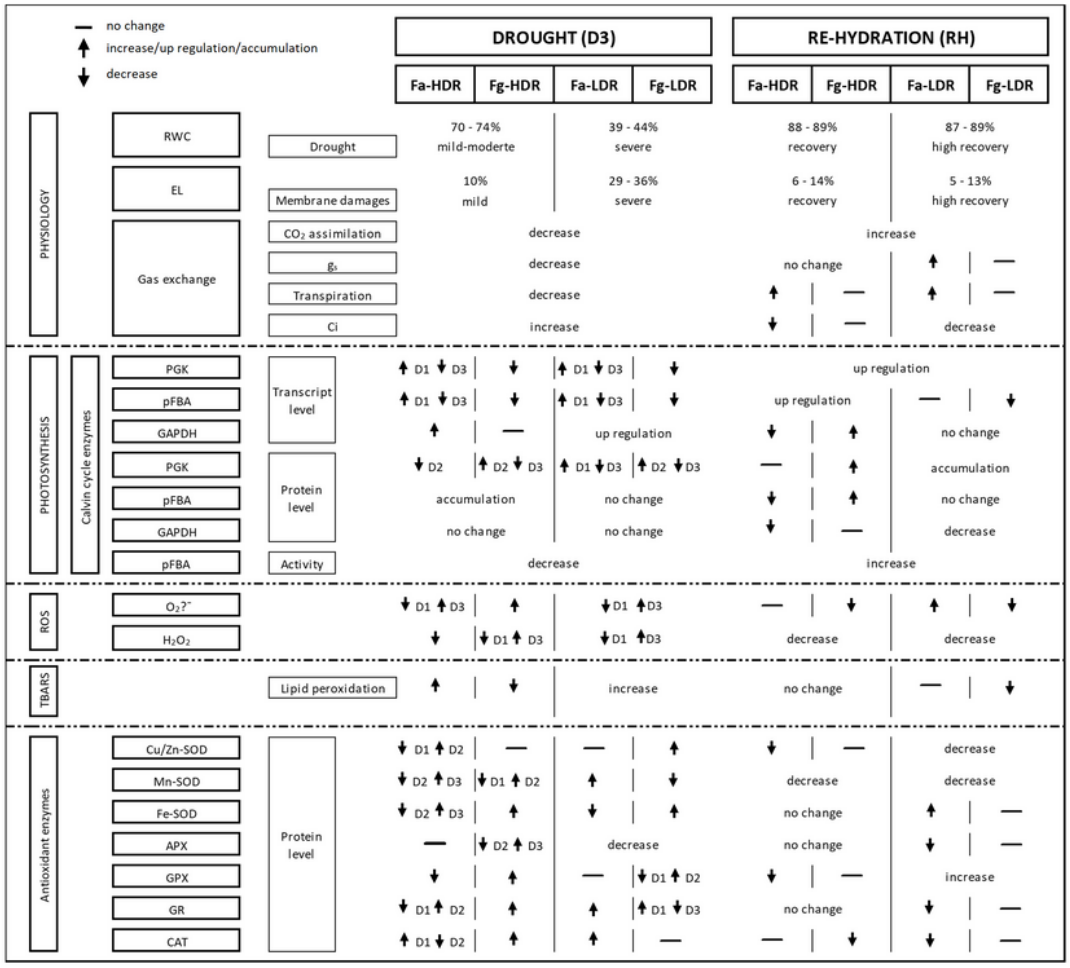

Figure 11

Comparison of physiological and molecular reactions in the HDR (Fa-HDR, Fg-HDR) and LDR (Fa-LDR, Fg-LDR) genotypes of F. arundinacea and F. glaucescens to drought stress on the 11th of water deficit (D3), unless otherwise stated; and after re-hydration (RH) in relation to D3.

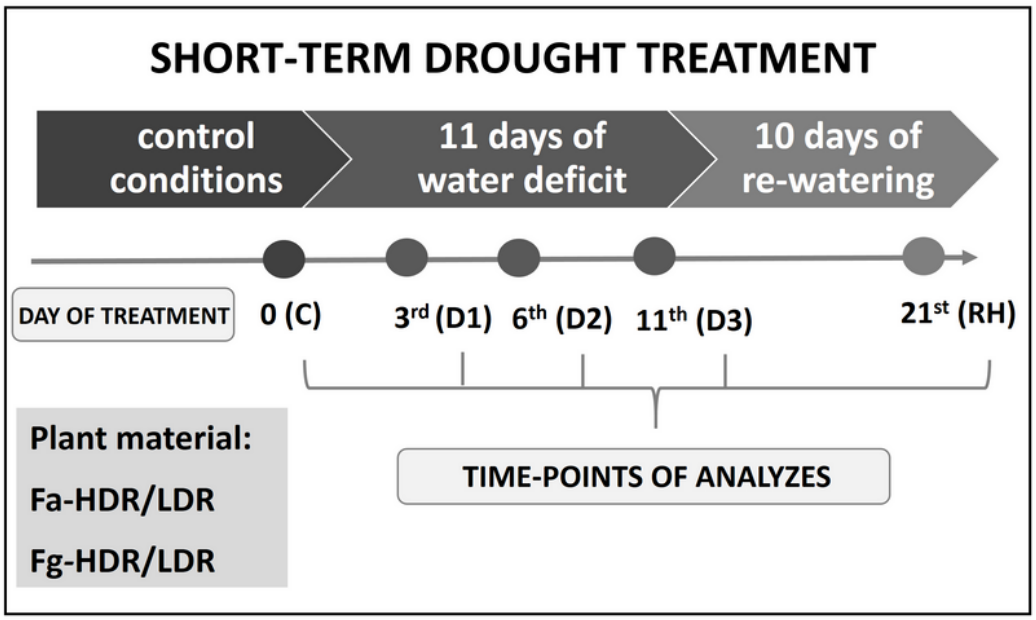

Figure 12

The scheme of short-term drought experiment performed with F. arundinacea and F. glaucescens

Supplementary Files

This is a list of supplementary files associated with this preprint. Click to download.

- Fig.S1.png
- Fig.S2.png